8

Extraction of Airway in Computed Tomography

Ken Inohara[1,2], Yuka I. Sumita[3] and Shuichi Ino[4]
[1]*University of Alberta*
[2]*Nihon University School of Dentistry*
[3]*Tokyo Medical and Dental University*
[4]*National Institute of Advanced Industrial Science and Technology*
[1]*Canada*
[2,3,4]*Japan*

1. Introduction

Computed tomography (CT) developed by Hounsfield (Hounsfield, 1973) extended the usefulness of radiography as a diagnostic technique. It enabled users to examine soft tissue in axial images, which previously had been limited mainly to hard tissue, e.g. bone and tooth. This was accomplished by the depiction of air space surrounding the soft tissue. Moreover, the development of high-speed scanning CT enabled three-dimensional observation of the anatomical structure of the human body. Slip-ring CT was developed by Toshiba in 1985 (Mori et. al., 1987) and by Siemens in 1987 (Kalender et. al., 1997), and Helical CT was in the practical application by the both companies in 1990 (Katakura, 1989) (Kalender et. al., 1990) (Kageyama et. al., 1992).
Furthermore, CT imaging in biomedical science has transcended its use as a diagnostic tool only. For example, three-dimensional reconstruction through rapid-prototyping techniques has been accomplished through application of CT imaging for novel use.
In this chapter, a standardized method for airway extraction from CT of the head and neck region is described. This process applies further to simulation of speech and swallowing, and for diagnosis of sleep apnea syndrome (SAS).

2. Airway extraction

2.1 Air as contrast material in general radiography and CT

The main target in general radiography is often hard tissues of the body such as bone and teeth. However, in some cases, air space can be taken as a contrast material when interested in the soft tissues of the body. Air encephalography was a typical example of instrumental assessment using air as contrast material before CT developed. This obsolete radiographic examination of the basal cisterns and ventricles of the brain was performed by filling the intracranial cerebrospinal fluid spaces with air, which was normally introduced through a lumbar puncture while the patient sat in an upright position. In chest radiography, air may be also used as a contrast material. For upper gastrointestinal tract radiography, a double contrast material (barium and air) method was developed by Shirakabe and Ichikawa (Kawai et. al., 1970), and is still widely used for cancer screening of stomach.
In CT examination, some methods using air as contrast material have been reported for exposure of the stomach and large intestine (Nagata et. al., 2004).

2.2 Extraction of airway in CT

In the head and neck region, photographs of air space were taken in early stages of CT development, especially exposure for diagnosis of SAS (Haponik et. al., 1983; Suratt et. al., 1983). However, there was a problem in that the conventional CT machine spent too much time to acquire images. As a solution, a slip-ring CT was developed and applied in the 1990s (Burger et. al., 1993). Additionally, trials for application of Helical CT have been performed (Lowe et. al., 1995).

In the field of phonetics, some studies using CT have been carried out for analysis of resonance characteristics of the vocal tract (airway). Story et al. investigated CT images of an adult woman's airway during vocalization to understand its transmission characteristics (Story et. al., 1998). Sundberg et al. took CT images of an opera singer during singing, followed by three-dimensional reconstruction for analysing the oropharyngeal shape (Sundberg et. al., 2007).

There is an important difference between surgical use and airway extraction in CT. The former is mainly for simulation which assists surgeons at operations by providing biomedical models. In the majority of cases, a main target of extraction from CT for biomedical modeling is hard tissue, mainly bone. In the field of head and neck defects, a prediction of facial change after sagittal splitting ramus osteotomy and a simulation of fibula grafting for resected mandible would be examples of use of such technology. Thus it permits a rough estimate of the outcome. However, the latter is for measurement of area and/or volume, thus it needs accuracy and reproducibility.

2.2.1 Determination of threshold

Determination of threshold is performed when converting CT images into binary values in order to measure volume of air space, followed by analysis of acoustical characteristics and diagnosing SAS (Fig. 1). It may seem that the threshold should be determined reasonably, but actually some difficulties exist.

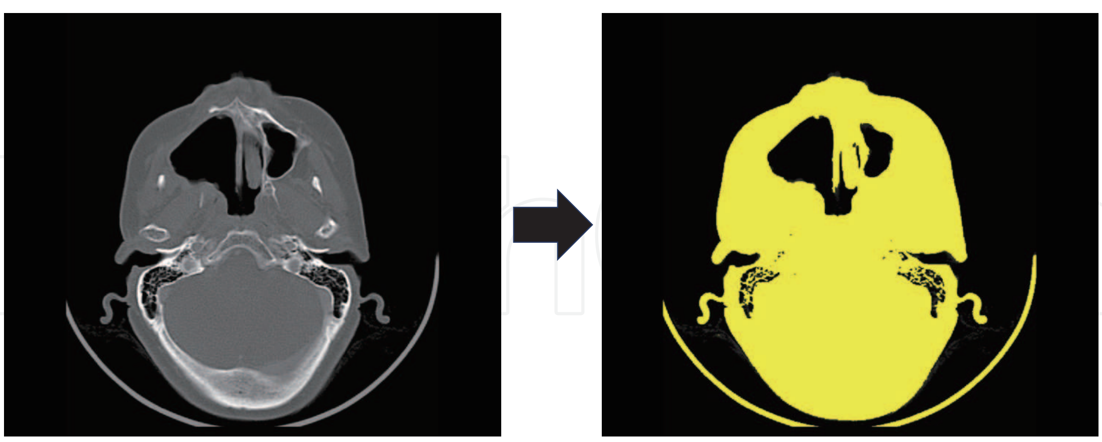

Fig. 1. An example of binary conversion.

2.2.2 Hounsfield number of air

The Hounsfield number (CT number) is a quantitative value for describing radiodensity. According to definition in Wikipedia, "The Hounsfield unit (HU) scale is a linear transformation of the original linear attenuation coefficient measurement into one in which the radiodensity of water is defined as 0 HU, while the radiodensity of air is defined as -1000

HU. For a material X with linear attenuation coefficient μ_x, the corresponding HU value is therefore given as below where μ_{water} and μ_{air} are the linear attenuation coefficients of water and air, respectively." (1)

$$HU = \frac{\mu_x - \mu_{water}}{\mu_{water} - \mu_{air}} \times 1000 \tag{1}$$

In biomedical engineering, 1024 (= 2^{10}) is usually substituted for 1000, thus the Hounsfield number of air should be -1024 HU.
According to the above definition, air space can be extracted when the threshold is set as -1024 HU. However, the area must be smaller than actual air space. Fig. 2 shows an example of vocal tract shape when threshold was set as -1024 HU. In the oropharynx region, the discontinuous form of the vocal tract was presented; this occurred because the air space was too small. This problem is known mainly as the "partial volume effect".

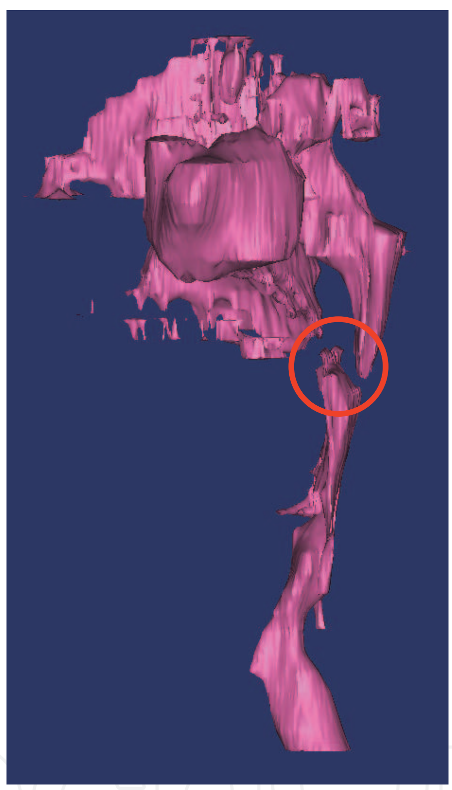

Fig. 2. A discontinuous vocal tract because of too low setting of threshold.

2.2.3 Pixel and voxel

Because one axial plane of the CT image generally consists of 512 x 512 pixels, minuteness of the image depends on the size of field of view (FOV) (Fig. 3).
In the case of 400 mm x 400 mm FOV, which is generally set in truncal imaging, the length of the side of the pixel is calculated as below (2).

$$400 \text{ mm} / 512 \text{ pixels} = 0.78125 \text{ mm} \tag{2}$$

With regard to the Z axis, it depends on the slice thickness/interval of imaging. The latest CT machines can take images in 0.5 mm or smaller intervals, but sometimes radiologists capture in thicker slices in order to reduce radiation to the patient.

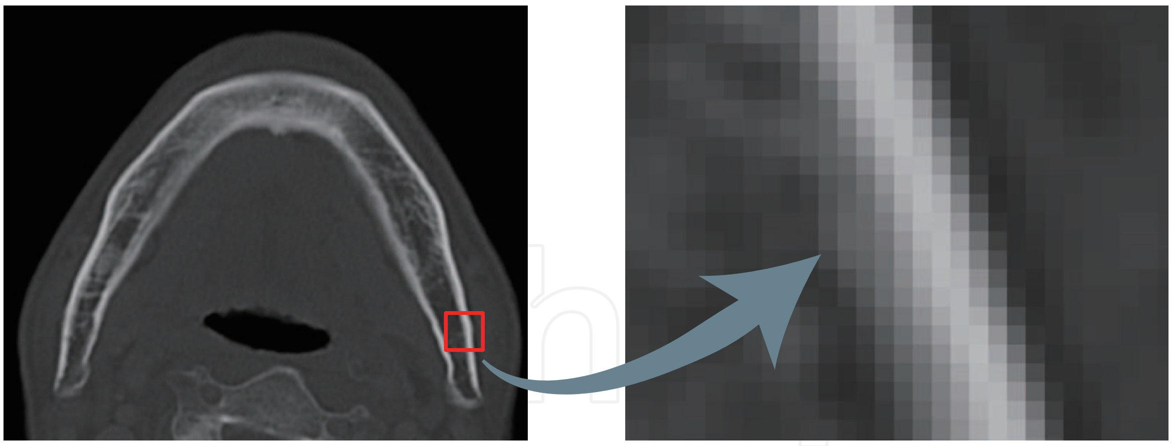

Fig. 3. Enlarged CT image (mandibular bone).

A rectangular prism with a pixel and Z axis slice thickness is named a "voxel" (Fig. 4). Three-dimensional CT data are an aggregate of voxels.

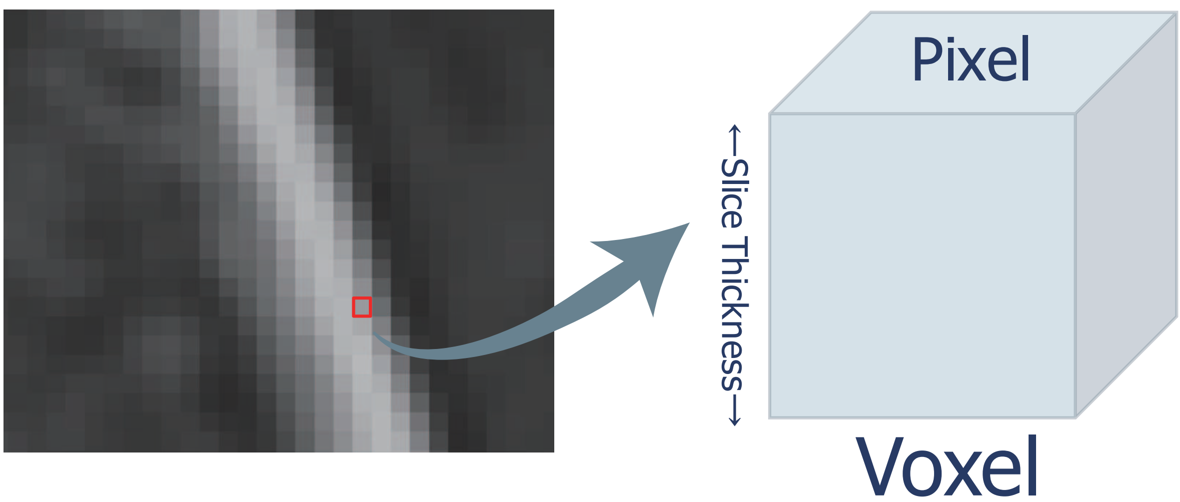

Fig. 4. Voxel is a rectangular prism with a pixel and slice thickness of Z axis.

2.2.4 Partial volume effect

The partial volume effect occurs when a single voxel contains a mixture of multiple tissue values. Each voxel has its own Hounsfield number. The Hounsfield number of the voxel at the boundary area between air and soft tissue is influenced by the both substances. (Fig. 5)
Following the definition of Hounsfield number, those of water and air are 0 HU and 1024 HU, respectively. However, the Hounsfield number of the internal air actually presents a higher value than 1024 HU. This is because of the partial volume effect, mentioned above. Therefore, we have to define precisely the threshold of Hounsfield number between soft tissue and air when images are converted into binary.
It means that setting of threshold influences the size of air space. For instance, when the Hounsfield number of a voxel is -600 HU and the threshold is set as -800 HU, the voxel may be judged as soft tissue. On the other hand, when the threshold is set as -500 HU, it may be as air. Thus, the area of air space can be changed to a couple of millimetres as setting of threshold easily, because the length of the side is approximately 0.5 to 2 mm that is depended on a voxel size (FOV and slice interval).

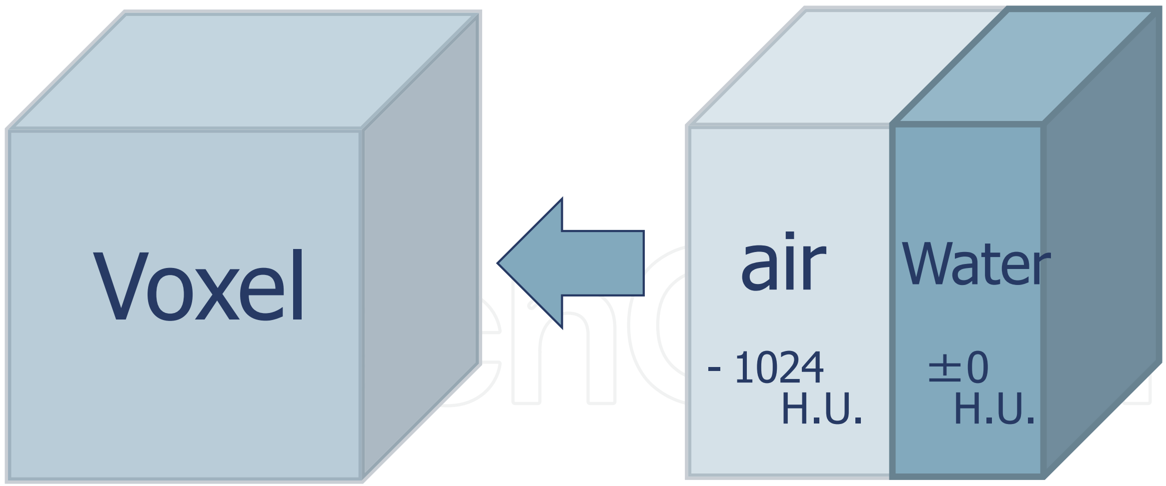

Fig. 5. Voxel contains a mixture of multiple tissue values.

In other research, the threshold generally has been decided by the operators' own subjective judgement, not in an objective way. Hence, the values have varied with different studies. It seems to be a serious problem for measuring size, area and/or volume, followed by transmission functions from data inaccuracy. Unfortunately, few studies have referred to the problem. For these reasons, standardized reconstruction methods have to be established.

3. Standardized airway extraction

In order to convert into binary objectively, standards must be set for thresholding. We noted that fat tissue has a Hounsfield number that is the lowest in human body. The following is a standardized method what we propose (Inohara et. al., 2010).

3.1 Hounsfield number of fat tissue

As described in formula (1), the Hounsfield number is a quantitative value for describing the radiodensity of each tissue of human body, where the radiodensity of water is 0 HU and that of air is -1024 HU. Fat tissue represents the lowest Hounsfield number in human body, which is approximately -80 HU. (Fig. 6)

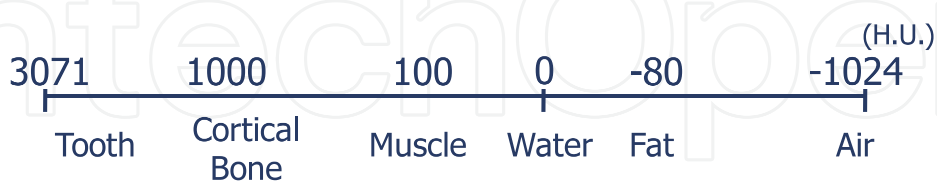

Fig. 6. Hounsfield value of each tissue of human body.

We hypothesized that objective binary conversion would be enabled by identification of the minimum setting of the Hounsfield value of fat tissue in the body. The Hounsfield number of fat tissue is generally said to be approximately -80 HU. However, the value has some spread-width actually. The optimal threshold value cannot exceed the minimum setting of fat tissue.

Fortunately, it is easy to find fat tissue, specifically the "Buccal fat-pad", in head and neck CT images for airway extraction. (Fig. 7)

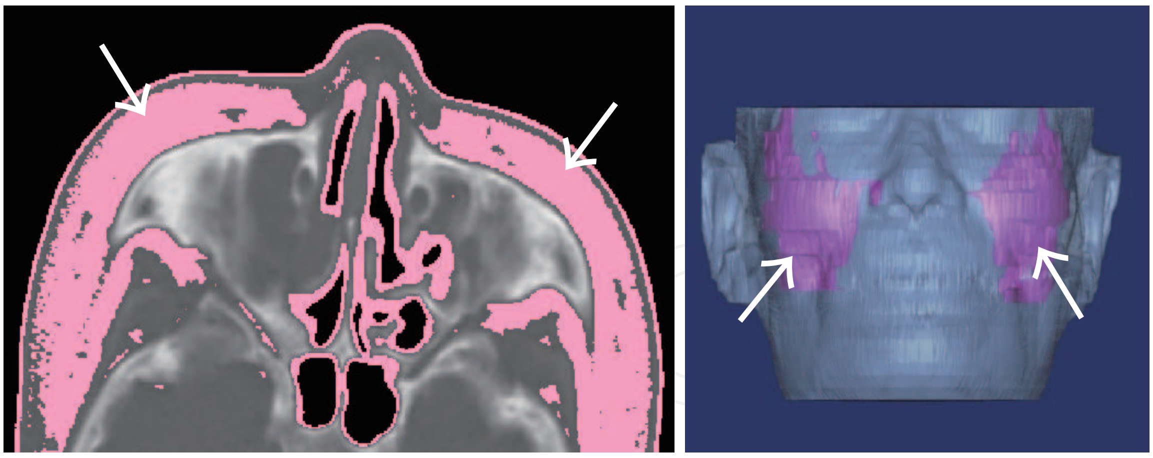

Fig. 7. Buccal fat-pad (arrow).

3.2 Detection of minimum setting of buccal fat-pad

To measure the bottom line of the Hounsfield number for the buccal fat-pad, a number of images that include the buccal fat-pad site should be examined. As the threshold value is down-regulated gradually, the voxels also decrease. The threshold value at which all representing voxels disappear in the images is the minimum setting of the buccal fat-pad. As an example, a process for detecting the minimum setting of Hounsfield value is shown in figure 8. In this subject, the minimum setting is determined as -247 HU. (Fig. 8)

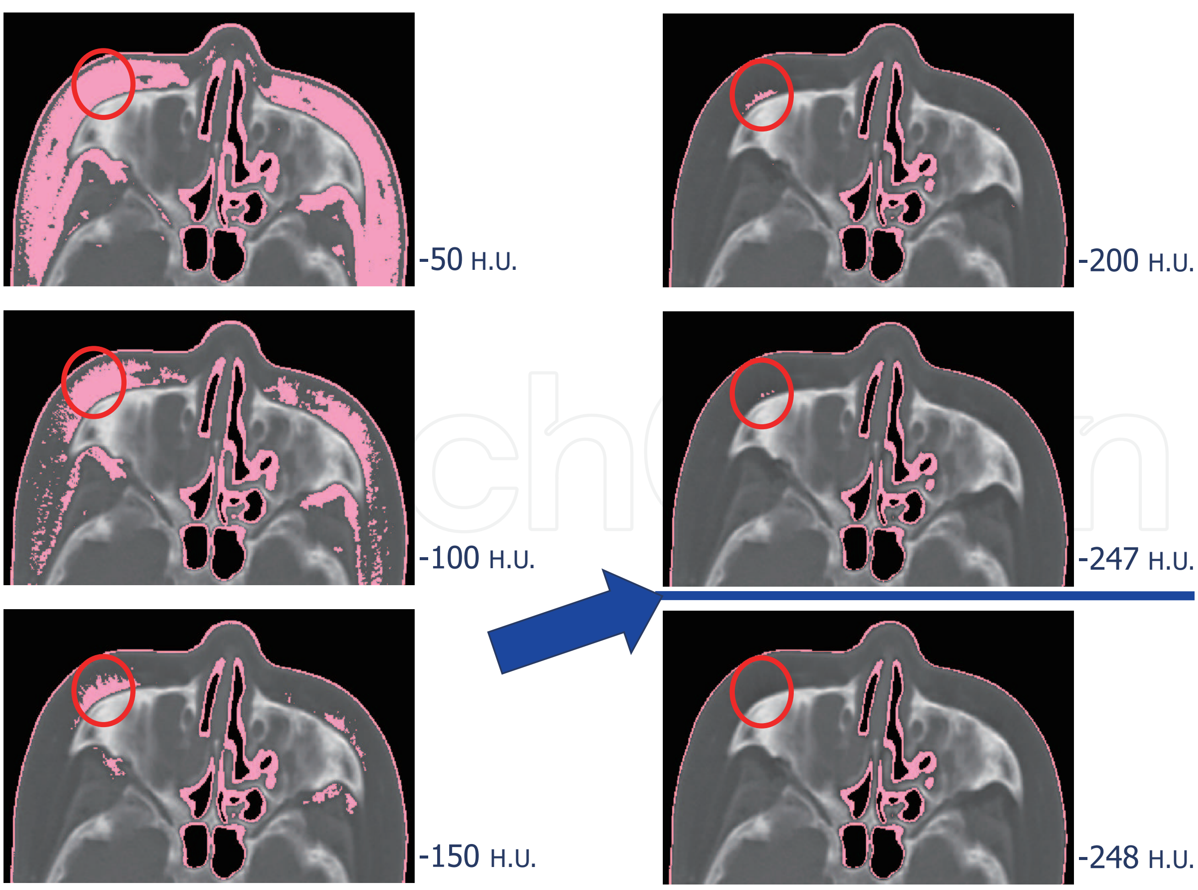

Fig. 8. Process of measuring minimum setting Hounsfield value of buccal fat-pad.

3.3 Evaluation of CT images in three-grade system

We describe the summary of process to determine the suitable threshold value on the following. The thresholds were set as the bottom line of the buccal fat-pad Hounsfield number, and the values of 50, 100, 150, 200, 250, and 300 HU were subtracted from the bottom line. (Fig.9)

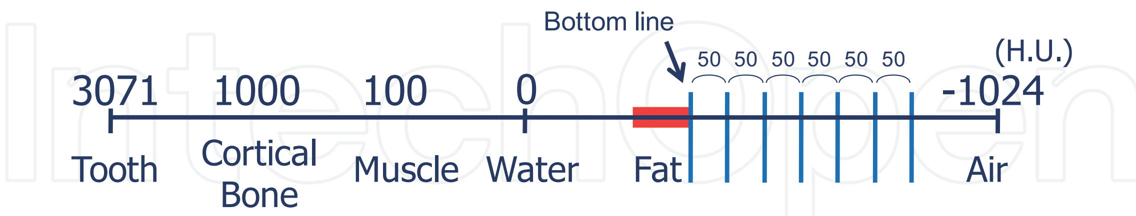

Fig. 9. Setting of threshold to evaluate images.

The regions where the structures were different among the thresholds were found in a series of each subject's images. In our previous study (Inohara et al, 2010) we evaluated the images as follows: G—the regions where the anatomical structure in the original images was revealed to be similar were judged to be good; NG—the regions where the structure was different from the original images were judged to be incorrect; P—the regions which came neither under G nor NG were judged passable. Following figure showed the judgment of nasal area. With regarding to turbinate and the nasal septum, the image that has separate parts is judged to be good (G), because the turbinate is generally separated from the nasal septum, because they should be actually separated in the normal human body. (Fig. 10)

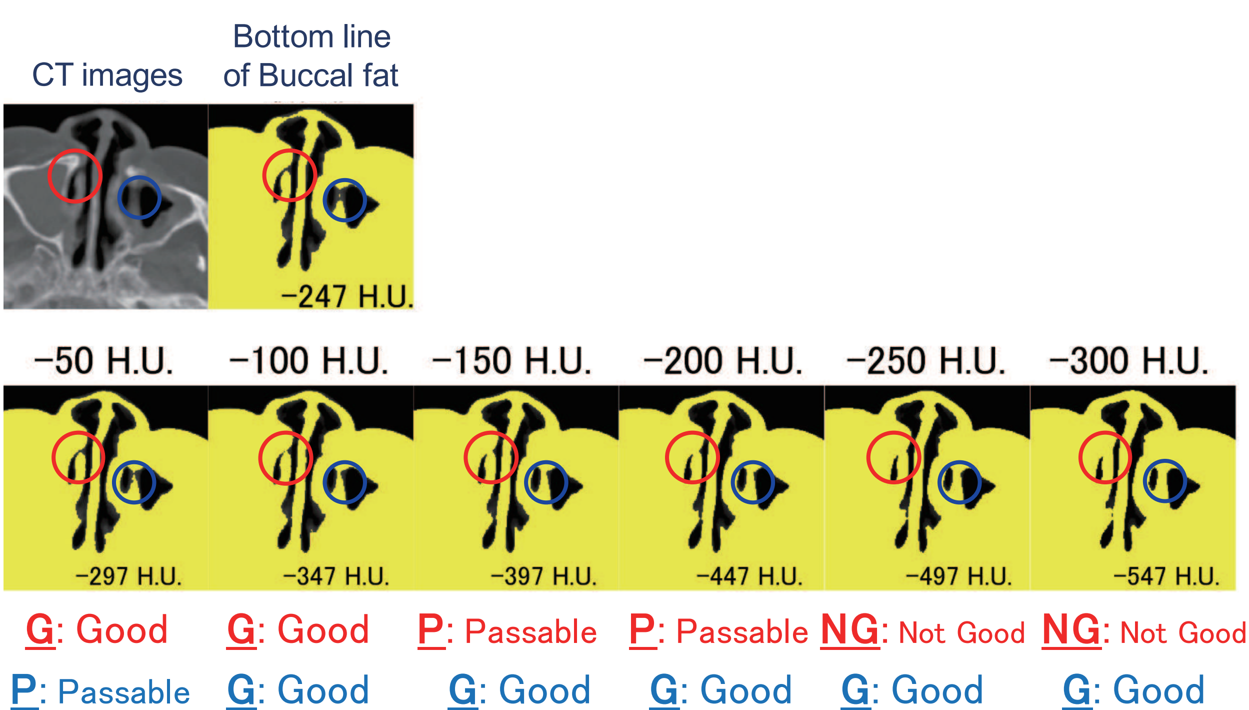

Fig. 10. An example of judgement by three-grade system.

In our study, five patients' CT images who had undergone maxillectomy of malignant tumors and had no resection of the zygomatic arch (because buccal fat pad was expected to be a criterion for thresholding) were employed. Slice distance of these images is 3 mm by

using a single-beam CT scanner. Data processing was performed by Mimics (Materialise NV, Belgium).
Each subject's G, P, and NG position numbers were counted and scored per the aforementioned thresholds as 2, 1, and -1 point respectively. Both positive and negative scores were summed as per the thresholds per subject, followed by being plotted on the graph. Regression analysis was performed, and the minimal Hounsfield value was calculated. (Fig. 11)

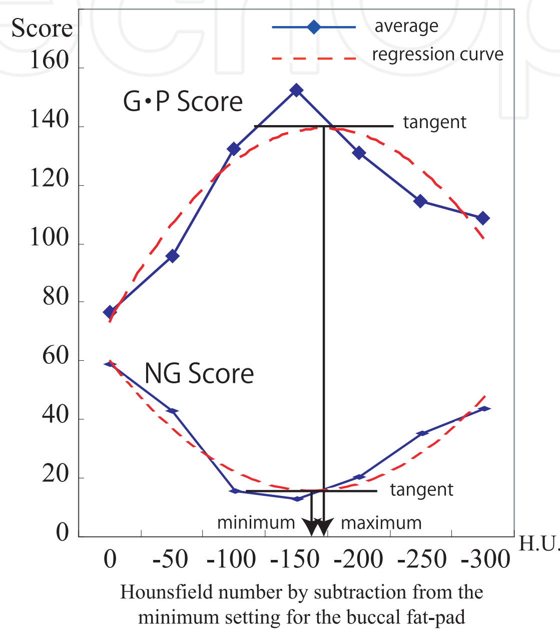

Fig. 11. Plot graphs of average scores, regression curves, tangents, and local maximum and minimum.

For the G and P positions (positive factor), the multiple regression equation (3) is as follows:

$$y = -9.40 \times 10^{-4}x - 2.25 \times 10^{-5}x^2 + 1.38 \quad (3)$$

As adjusted R^2 = 0.855, fitness is good. As significance probability of the binomial term was p = 0.012 and the sign was negative, this regression curve was convex upward. The local maximal was the minimum setting of -170 HU.
For the NG positions (negative factor), the multiple regression equation (4) is as follows:

$$\mathrm{y} = 4.10 \times 10^{-4}\mathrm{x} + 1.72 \times 10^{-5}\mathrm{x}^2 + 0.164 \quad (4)$$

As adjusted R^2 = 0.866, fitness is good. As significance probability of the binomial term was p = 0.004 and the sign is positive, this regression curve was convex downward. The local minimum was the minimum setting of -161 HU. From these results, the optimal threshold as -165 HU from each patient's minimum values of the buccal fat-pad region was deduced in our previous study.

3.4 Verification of the standardized method

As mentioned above, first, we hypothesized that objective binary conversion would be enabled by identification of the minimum setting of the Hounsfield value of fat tissue in the body. The minimum setting of the buccal fat-pad could be clearly measured individually, which varied between approximately -200 and -310 HU. This result is explainable because the Hounsfield value of each tissue has some spread-width actually, although the value of fat tissue is generally said to be approximately -80 HU.

Optimal threshold value could be calculated objectively by applying anatomical and statistical analysis. We have built a solid model of the vocal tract by the aforementioned method to confirm accuracy of the method what we proposed. (Fig. 12)

We have already started new research by using these models to disclose transmission characteristics of patients with surgical resection in the head and neck.

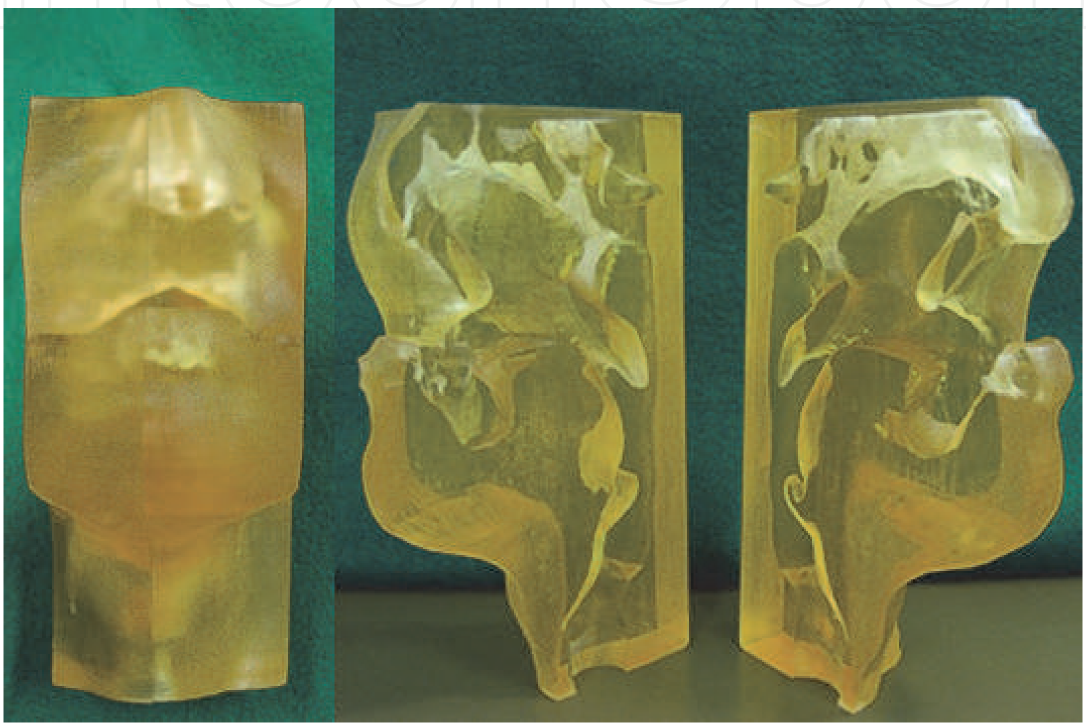

Fig. 12. A model reconstructed by rapid prototyping what applied the standardized method

4. Future of airway extraction

The use of CT imaging in biomedical science has been developing rapidly, transcending its use as a diagnostic tool only. Three-dimensional reconstruction and rapid-prototyping, enabled by CT imaging, are particularly important in the field of biomedical science. The field of air extraction benefits from development of biomedical science.

Our main interest is the shape of the vocal tract during phonation, especially head and neck cancer patients. (Fig. 13) The standardized method of airway extraction that we proposed can contribute to accuracy of measuring and analysis.

Technology of airway extraction in CT is applied in various diagnostic and research scenes, especially for SAS patients. For instance, there is a study to assess the predictive power of an otorhinolaryngological examination of the upper airway to identify risk factors of SAS in the patients (Yagi et. al., 2009). In addition, there is research about airway obstruction in infants with a hypoplastic mandible (Looby et. al., 2009).

Moreover, some recent studies have been performed by using four-dimensional reconstruction in multi detector-row CT (MDCT); this means using dynamic images, especially in a field of swallowing assessment. Although videofluorography with a modified barium swallowing test (Martin-Harris et. al., 2000) is applied generally in dysphagia assessment, there is risk of aspiration, followed by pneumonia. To avoid this risk, research has been performed where a subject swallowed just air, captured by a 64-row MDCT that is generally used for cardiac cine-CT (Fudeya et. al., 2010). In addition, there is recent research of applying 320-row MDCT, which is the most up-to date facility (Inomoto et. al., 2010).

Fig. 13. Examination of analysis of vocal tract transmission characteristics using a model that was rapid-prototyped by our proposed method.

5. Conclusion

In this chapter, the standardized method for airway extraction was described in detail. As the necessity of airway extraction in CT is now increasing, establishment of a standardized method for air extraction is needed. The method that we proposed is simple, objective, and effective.

6. Acknowledgements

This work was partially supported by the Grant-in-Aid for Young Scientist (B), the Ministry of Education, Culture, Sports, Science and Technology, Japan (MEXT Grant). The authors would like to thank for Ms. L. Dunwald in Misericordia Community Hospital, Drs. H. Taniguchi, T. Kurabayashi, N. Ohbayashi in Tokyo Medical and Dental University, T. Ifukube in University of Tokyo, and J. Rieger in University of Alberta.

7. References

Burger, C. D.; Stanson, A. W.; Daniels, B. K.; Sheedy, P. F. & Shepard, J. W. (1993). Fast-computed tomographic evaluation of the effect of route of breathing on upper airway size and function in normal men. *Chest*, Vol. 103, No. 4, pp. 1032-1037

Fudeya, T.; Otake, S.; Watabe, H.; Mitsuoka, T. & Yoshikawa, A. (2010). Visualization of laryngopharynx during swallowing of negative contrast media (air) with cine mode 64-row MDCT. *Nippon Hoshasen Gijutsu Gakkai Zasshi*, Vol. 66, No. 5, pp. 535-539

Haponik, E. F.; Smith, P. L.; Bohlman, M. E.; Allen, R. P. & Goldman, S. M. (1983). Computerized tomography in obstructive sleep apnea. Correlation of airway size with physiology during sleep and wakefulness. *American Review of Respiratory Disease*, Vol. 127, No. 2, pp. 221-226

Hounsfield, G. N. (1973). Computerized transverse axial scanning (tomography) .1. description of system. *British Journal of Radiology*, Vol. 46, No. 552, pp. 1016-1022

Inohara, K,; Sumita, Y. I.; Ohbayashi, N.; Ino, S.; Kurabayashi, T.; Ifukube, T. & Taniguchi, H. (2010). Standardization of thresholding for binary conversion of vocal tract modeling in computed tomography. *Journal of Voice*, Vol. 24, No. 4, pp. 503-509

Inamoto, Y.; Fujii, N.; Saitoh, E.; Baba, M.; Okada, S.; Katada, K.; Ozeki, Y.; Kanamori D. & Palmer, J.B. (2010). Evaluation of swallowing using 320-detector-row multislice 16 CT. Part II: Kinematic analysis of laryngeal closure during normal swallowing. *Dysphagia*, DOI : 10.1007/s00455-010-9276-2

Kageyama, K.; Kimura, K.; Katakura, T.; Suzuki, K.; Aizumi, J. & Seino, O. (1992). Helical volume CT and its clinical significance. *Fukushima Journal of Medical Science*, Vol. 38, No. 2, pp. 67-74

Kalender, W. A.; Engelke, K. & Schaller, S. (1997). Spiral CT: medical use and potential industrial applications. *SPIE*, Vol. 3149, pp. 188-202

Kalender, W. A.; Seissler, W.; Klotz, E. & Vock, P. (1990). Spiral volumetric CT with single-breath-hold technique, continuous transport, and continuous scanner rotation. *Radiology*, Vol. 176, No. 1, pp. 181-183

Katakura, T. (1989). Basic research of Computed Tomography (IX) - Helical CT scanner. *Dansou Eizou Kenkyukai Zasshi*, Vol. 16, pp. 247-250

Kawai, K.; Takada, H.; Takekoshi, T.; Misaki, F.; Murakami, K.; Masada, M.; Nishizawa, M.; Hayakawa, H. & Shirakabe, H. (1970). Double contrast radiograph on routine examination of the stomach. *American Journal of Gastroenterology*, Vol. 53, No. 2, pp. 147-153

Looby, J. F.; Schendel, S. A.; Lorenz, H. P.; Hopkins, E. M. & Aizenbud, D. (2009). Airway analysis: with bilateral distraction of the infant mandible. *Journal of Craniofacial Surgery*, Vol. 20, No. 5, pp. 1341-1346

Lowe, A. A.; Fleetham, J. A.; Adachi, S. & Ryan, C. F. (1995). Cephalometric and computed tomographic predictors of obstructive sleep apnea severity. *American Journal of Orthodontics and Dentofacial Orthopedics*, Vol. 107, No. 6, pp. 589-595

Martin-Harris, B.; Logemann, J. A.; McMahon, S.; Schleicher, M. & Sandidge, J. (2000). Clinical utility of the modified barium swallow. *Dysphagia*, Vol. 15, No. 3, pp. 136-141

Mori, K.; Saito, K. & Asahina, K. (1987). X-ray CT TCT-900S. *Toshiba review*, Vol. 42, No. 2, pp. 80-82

Nagata, K.; Endo, S.; Kudo, S.; Kitanosono, T. & Kushihashi, T. (2004). CT air-contrast enema as a preoperative examination for colorectal cancer. *Digestive Surgery*, Vol. 21, No. 5-6, pp. 352-358

Story, B. H.; Titze, I. R. & Hoffman, E. A. (1998). Vocal tract area functions for an adult female speaker based on volumetric imaging. *Journal of the Acoustical Society of America*, Vol. 104, No. 1, pp. 471-487

Sundberg, J.; Birch, P.; Gumoes, B.; Stavad, H.; Prytz, S. & Karle, A. (2007). Experimental findings on the nasal tract resonator in singing. *Journal of Voice*. Vol. 21, No. 2, pp. 127-137

Suratt, P. M.; Dee, P.; Atkinson, R. L.; Armstrong, P. & Wilhoit, S. C. (1983). Fluoroscopic and computed tomographic features of the pharyngeal airway in obstructive sleep apnea. *American Review of Respiratory Disease*, Vol. 127, No. 4, pp. 487-492

Yagi, H.; Nakata, S.; Tsuge, H.; Yasuma, F.; Noda, A.; Morinaga, M.; Tagaya, M. & Nakashima, T. (2009). Morphological examination of upper airway in obstructive sleep apnea. *Auris Nasus Larynx*, Vol. 36, No. 4, pp. 444-449

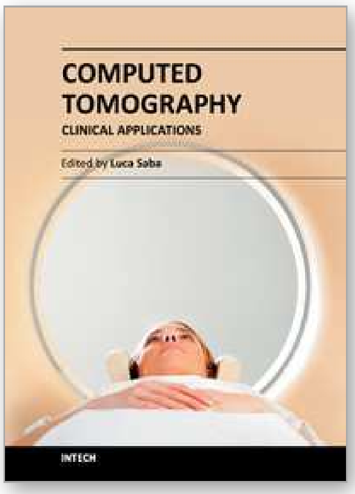

Computed Tomography - Clinical Applications
Edited by Dr. Luca Saba

ISBN 978-953-307-378-1
Hard cover, 342 pages
Publisher InTech
Published online 05, January, 2012
Published in print edition January, 2012